

Properties of the relaxation time distribution underlying the Kohlrausch–Williams–Watts photoionization of the DX centers in $\text{Cd}_{1-x}\text{Mn}_x\text{Te}$ mixed crystals

This article has been downloaded from IOPscience. Please scroll down to see the full text article.

2009 J. Phys.: Condens. Matter 21 345801

(<http://iopscience.iop.org/0953-8984/21/34/345801>)

View [the table of contents for this issue](#), or go to the [journal homepage](#) for more

Download details:

IP Address: 129.252.86.83

The article was downloaded on 29/05/2010 at 20:47

Please note that [terms and conditions apply](#).

Properties of the relaxation time distribution underlying the Kohlrausch–Williams–Watts photoionization of the DX centers in $\text{Cd}_{1-x}\text{Mn}_x\text{Te}$ mixed crystals

J Trzmiel¹, K Weron¹, J Janczura² and E Placzek-Popko¹

¹ Institute of Physics, Wrocław University of Technology, Wybrzeże Wyspińskiego 27, 50-370 Wrocław, Poland

² Hugo Steinhaus Center for Stochastic Methods and Institute of Mathematics and Computer Science, Wrocław University of Technology, Wybrzeże Wyspińskiego 27, 50-370 Wrocław, Poland

Received 5 May 2009, in final form 18 July 2009

Published 5 August 2009

Online at stacks.iop.org/JPhysCM/21/345801

Abstract

In this paper we clarify the relationship between the relaxation rate and relaxation time distributions underlying the Kohlrausch–Williams–Watts (KWW) photoconductivity build-ups in indium- and gallium-doped $\text{Cd}_{1-x}\text{Mn}_x\text{Te}$ mixed crystals. We discuss the role of asymptotic properties of the corresponding probability density functions. We show that the relaxation rate distribution, as a completely asymmetric α -stable distribution, leads to an infinite mean value of the effective relaxation rate. In contrast, the relaxation time distribution related to it leads to a finite mean value of the effective relaxation time. It follows from the experimental data analysis that for all the investigated samples the KWW exponent α decreases linearly with increasing photon flux in the range of (0.6–0.99) and its values are more spread in the case of gallium-doped material. We also observe a linear dependence of the mean relaxation time on the characteristic material time constant, which is consistent with the theoretical model.

1. Introduction

For many years relaxation processes were a subject of intensive investigations. These studies revealed that a wide class of various materials, e.g. amorphous and crystalline semiconductors, insulators, polymers, disordered crystals, molecular solid solutions and glasses, exhibit non-exponential relaxation patterns. It has been stated that, regardless of the relaxing medium the empirically observed relaxation patterns reflect some universal behavior of the investigated system. It was found that the relaxation responses obtained by different experimental techniques can be well characterized by a small class of fitting functions exhibiting asymptotically power-law properties [1–3].

The most popular function applied to fit the time-domain relaxation data is the stretched-exponential function, known

also as the Kohlrausch–Williams–Watts (KWW) function:

$$\Phi_{\text{KWW}}(t) = e^{-(At)^\alpha}, \quad (1)$$

where $0 < \alpha < 1$ is the stretching exponent and A is an inverse of the characteristic material time constant. The corresponding response function, i.e. the negative time derivative of the KWW function, exhibits the short-time power-law property and decays stretched-exponentially for long times:

$$f_{\text{KWW}}(t) = -\frac{d\Phi_{\text{KWW}}(t)}{dt} \propto \begin{cases} t^{\alpha-1}, & t \rightarrow 0 \\ e^{-(At)^\alpha}, & t \rightarrow \infty. \end{cases} \quad (2)$$

Until the development of stochastic approaches to relaxation, the origins of such response characteristics remained unclear. Fortunately, the recent progress in stochastic modeling [4–8] allows us to disclose physical mechanisms

responsible for the above asymptotic property of the KWW fitting function.

It has been reported in [9, 10] that persistent photoconductivity build-up in semiconducting multiterinary alloys possessing metastable defects called DX centers follows the non-exponential relaxation pattern and can be properly described using the KWW function. It has been shown that the detected KWW type of measured responses results from a heavy-tailed distribution of the DX centers' relaxation rates [11]. The aim of this paper is to clarify the properties of the relaxation time distribution underlying the KWW photoionization of the DX centers in indium- and gallium-doped $\text{Cd}_{1-x}\text{Mn}_x\text{Te}$ mixed crystals. The proposed approach gives a deeper insight into the non-exponentiality of photoconductivity build-ups in the studied materials.

2. Mathematical description of stretched-exponential relaxation processes

According to the historically oldest approach to relaxation, a macroscopic non-exponential time-domain relaxation response results from a classical (exponential) Debye process with different relaxation times [12]. As a consequence the non-exponential relaxation function can be mathematically expressed as a weighted average of an exponential decay $e^{-t/\tau}$ with respect to the distribution $g(\tau) d\tau$ of the random effective relaxation time T :

$$\Phi(t) = \langle e^{-t/T} \rangle. \quad (3)$$

The above formula reflects stochastic properties of the considered physical system as a whole. It is a well-known fact of probability theory [13] that the average (3) can be expressed in the integral form

$$\Phi(t) = \langle e^{-t/T} \rangle = \int_0^\infty e^{-t/\tau} g(\tau) d\tau, \quad (4)$$

if the random relaxation time T takes values τ from the range $[0, \infty)$ with probability $g(\tau) d\tau$, where $g(\tau)$ is the effective relaxation time probability density function (pdf).

The relaxation function can also be expressed by means of the random relaxation rate $\beta = 1/T$ taking values b from the range $[0, \infty)$. Formula (4) can then be rewritten into an equivalent form:

$$\Phi(t) = \langle e^{-\beta t} \rangle = \int_0^\infty e^{-bt} \rho(b) db, \quad (5)$$

where $\rho(b)$ denotes now the effective relaxation rate pdf. In the above formula the relaxation function $\Phi(t)$, as the exponentially weighted mean value of the effective relaxation rate β , is simply expressed by means of the Laplace transform of the relaxation rate pdf $\rho(b)$. It follows from [5–8] that such a representation allows a better understanding of the stochastic mechanism underlying the non-exponential relaxation. Both probability density functions (cf equations (4) and (5)) are interrelated. The relationship between them is given by the formula

$$\rho(b) = \frac{1}{b^2} g\left(\frac{1}{b}\right). \quad (6)$$

Using the notion of the random relaxation rate β the stretched-exponential relaxation function (1) may be expressed as

$$\Phi_{\text{KWW}}(t) = e^{-(At)^\alpha} = \langle e^{-\beta_{\text{KWW}} t} \rangle = \int_0^\infty e^{-bt} \rho_{\text{KWW}}(b) db. \quad (7)$$

Thus the relaxation function $\Phi_{\text{KWW}}(t)$ is expressed as the Laplace transform of the relaxation rate pdf $\rho_{\text{KWW}}(b)$. It has been shown in [4–8] that β_{KWW} is an α -stable, non-negative random variable possessing the completely asymmetric α -stable pdf [14]. In general, the explicit form of the completely asymmetric α -stable densities is unknown. It can, however, be expressed by means of the series representation [14], namely we have

$$\rho(b) = \left[\frac{B(\alpha)\lambda(\alpha)}{2\pi(1-\alpha)} \right]^{\frac{1}{\alpha}} \left(\frac{b}{\gamma} \right)^{-\frac{\lambda(\alpha)}{2}} \frac{1}{b} \times \exp\left[-B(\alpha) \left(\frac{b}{\gamma} \right)^{-\lambda(\alpha)} \right], \quad \text{for } b \rightarrow 0 \quad (8)$$

where

$$B(\alpha) = (1-\alpha)\alpha^{\frac{\alpha}{1-\alpha}} \left(\cos\left(\frac{\pi\alpha}{2}\right) \right)^{-\frac{1}{1-\alpha}}, \quad \lambda(\alpha) = \frac{\alpha}{1-\alpha}$$

and

$$\rho(b) = \frac{1}{\pi b} \sum_{n=1}^{\infty} (-1)^{n+1} \frac{\Gamma(n\alpha+1)}{n!} \left[\left(\cos\left(\frac{\pi\alpha}{2}\right) \right)^{\frac{1}{\alpha}} \frac{b}{\gamma} \right]^{-n\alpha} \times \sin(n\pi\alpha), \quad \text{for } b \rightarrow \infty \quad (9)$$

where $\gamma[\text{s}^{-1}] > 0$ is some fixed positive constant and $\Gamma(\cdot)$ signs the gamma function. For $b \rightarrow 0$ the behavior of the α -stable pdf $\rho(b)$ is dominated by the term $\exp[-B(\alpha)(b/\gamma)^{-\lambda(\alpha)}]$ whereas for $b \rightarrow \infty$ the relaxation rate pdf exhibits the power-law properties. The asymptotic properties of the relaxation rate pdf are directly related to the asymptotic behavior of its Laplace transform. It is a well-known fact that the properties of a function $p(x)$ for $x \rightarrow \infty$ correspond to the properties of its Laplace transform $L(p(x), t)$ for $t \rightarrow 0$. The Tauberian theorems [13] imply then that the short-time power law $t^{\alpha-1}$ of the KWW response function $f_{\text{KWW}}(t)$, see equation (2), follows from the power-law tail property

$$\rho_{\text{KWW}}(b) \propto b^{-\alpha-1}, \quad 0 < \alpha < 1, \quad b \rightarrow \infty \quad (10)$$

of the relaxation rate pdf for large b . It is clear from probability theory that the KWW relaxation rate, distributed according to the distribution with the tail property (10), cannot lead to the finite mean value of the effective relaxation rate, i.e.

$$b_{\text{KWW}} = \langle \beta_{\text{KWW}} \rangle = \int_0^\infty b \rho_{\text{KWW}}(b) db = \infty. \quad (11)$$

Property (10) denotes that the effective rate distribution in the KWW relaxation pattern is scale-invariant. The distribution looks the same at each length scale, i.e. it is not possible to define a characteristic macroscopic rate, as it may with the same probability take both large and small values.

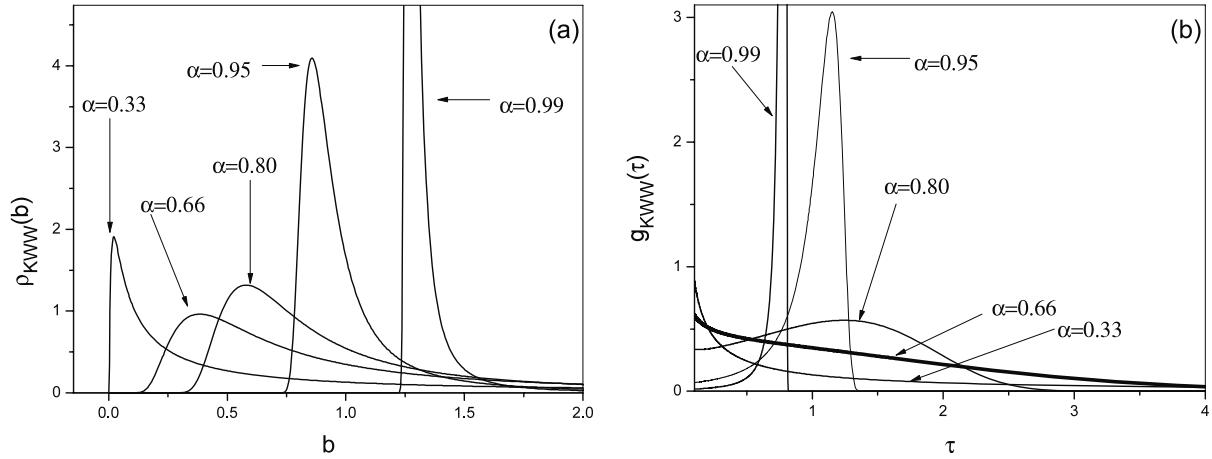


Figure 1. The KWW relaxation rate (a) and relaxation time (b) probability density functions calculated for various values of the stretching exponent α .

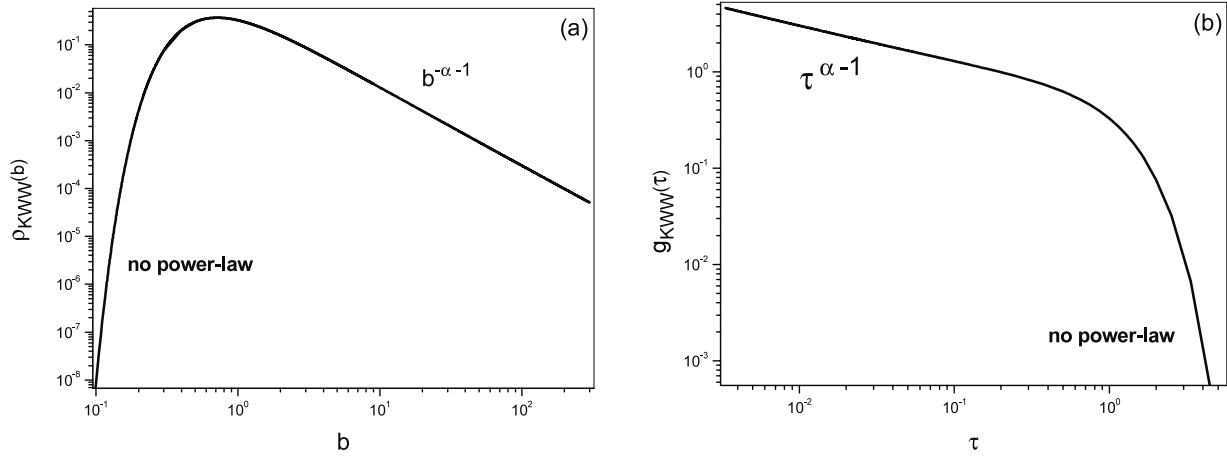


Figure 2. The log–log plot of the KWW relaxation rate (a) and relaxation time (b) probability density functions for the stretching exponent $\alpha = 0.6$.

Due to the fact that $\rho_{KWW}(b)$ and $g_{KWW}(\tau)$ are related by equation (6), we get

$$g_{KWW}(\tau) = \frac{1}{\tau^2} \rho_{KWW}\left(\frac{1}{\tau}\right), \quad (12)$$

from which one can easily obtain that the power-law asymptotic behavior of $\rho_{KWW}(b)$ for large b yields the following dependence of $g_{KWW}(\tau)$:

$$g_{KWW}(\tau) \propto \tau^{\alpha-1}, \quad \tau \rightarrow 0. \quad (13)$$

In contrast to the KWW relaxation rate pdf $\rho_{KWW}(b)$, the relaxation time distribution $g_{KWW}(\tau)$ does not exhibit the power-law tail for large τ . Thus, the relaxation time distribution allows us to calculate the finite mean value of the random effective relaxation time T :

$$\tau_{KWW} = \langle T_{KWW} \rangle = \int_0^\infty \tau g_{KWW}(\tau) d\tau < \infty. \quad (14)$$

In figure 1 samples of the KWW relaxation rate and relaxation time pdfs calculated for various values of the

stretching exponent α are plotted. In the limiting case, when α tends to 1, the densities tend to δ -Dirac function. Note that relaxation rate pdfs are unimodal, regardless of the value of α whereas relaxation time pdfs are unimodal solely, when $\alpha > \frac{2}{3}$. For $\alpha \leq \frac{2}{3}$, the densities are monotonically decaying. In figure 2 the sample relaxation rate and relaxation time density pdfs for $\alpha = 0.6$ are presented in a log–log scale. It is clear from the plot that both the densities exhibit different asymptotic properties.

3. Experiment

Single crystals of $\text{Cd}_{0.93}\text{Mn}_{0.07}\text{Te:In}$, $\text{Cd}_{0.9}\text{Mn}_{0.1}\text{Te:In}$ and $\text{Cd}_{0.99}\text{Mn}_{0.01}\text{Te:Ga}$, grown by the Bridgman method, were used for this study. Prior to the measurements the samples were annealed in cadmium vapor to reduce the cadmium vacancies. Slices of the material were mechanically polished and etched in a 2% Br_2 in methanol solution. Capacitance–voltage measurements performed with a 1 MHz capacitance bridge yielded the room temperature donor net concentration

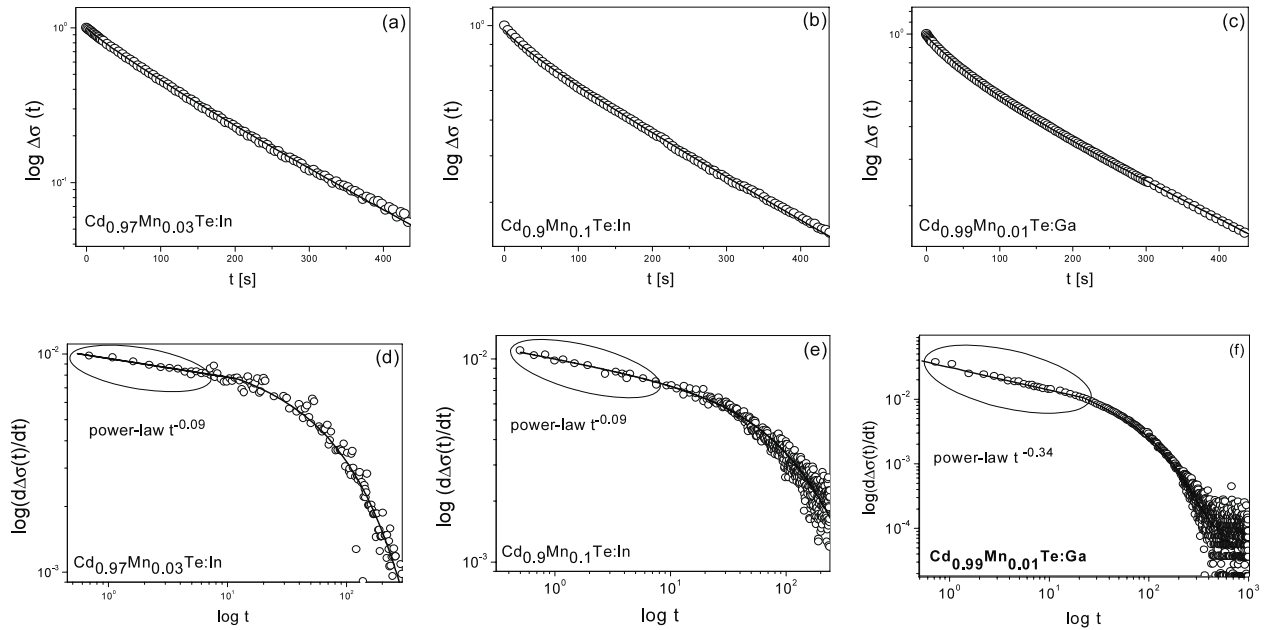


Figure 3. The transient of the normalized relative photoconductivity (relaxation data) and the negative time derivative of the transient (response data) for indium- and gallium-doped $\text{Cd}_{1-x}\text{Mn}_x\text{Te}$. The kinetics were recorded at 77 K for 1.24 eV photon energy, under the same illumination conditions. The solid lines are the best fits of the stretched-exponential function (1) to the measured data.

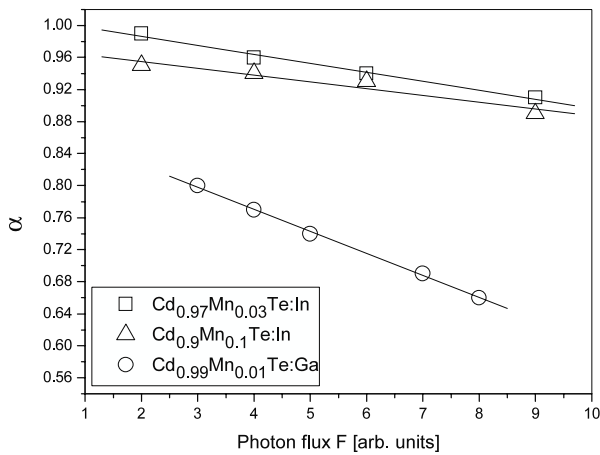


Figure 4. Stretching exponent versus photon flux plot. For all the samples under study α decreases with increasing photon flux.

of the order of 10^{15} cm^{-3} for $\text{Cd}_{0.93}\text{Mn}_{0.07}\text{Te}$:In and 10^{16} cm^{-3} for $\text{Cd}_{0.9}\text{Mn}_{0.1}\text{Te}$:In and $\text{Cd}_{0.99}\text{Mn}_{0.01}\text{Te}$:Ga samples.

For the photoconductivity measurements, ohmic contacts were made by indium soldering of gold wires to fresh surfaces of the wafers. The four-point probe method was utilized. In the experiment, the measurement of potential difference across the sample was carried out at 10 μA current supplied from a Keithley constant-current source. A tungsten lamp served as a light source for illumination of the sample and a shutter with a 0.2 s time constant was used to turn the light on and off. The light passed through a monochromator and with the help of fiber optics the monochromatic beam was focused on the sample immersed in liquid nitrogen. A thermopile was used to measure the light intensity.

All photoconductivity transients were recorded at 77 K after exposing the samples to monochromatic light with photon energy equal to 1.24 eV. This energy is less than the bandgap in the investigated materials. The measurements were carried out at various photon fluxes. Prior to each measurement, the investigated sample had to be warmed up to a temperature at which persistent photoconductivity was suppressed. Subsequently, the sample was cooled down in darkness to liquid nitrogen temperatures. Under illumination, the measurement was carried out until conductivity was saturated. Typically the build-up of conductivity lasted several minutes.

4. Results and discussion

It has been stated that photoconductivity build-ups in $\text{Cd}_{1-x}\text{Mn}_x\text{Te}$:In and $\text{Cd}_{1-x}\text{Mn}_x\text{Te}$:Ga exhibit the KWW relaxation pattern [9, 10]. In figures 3(a)–(c), the kinetics of photoconductivity build-up at 77 K, obtained for the investigated samples, are depicted. The normalized relative change $\Delta\sigma(t)$ in the conductivity due to illumination:

$$\Delta\sigma(t) = \frac{\sigma(t_{\text{sat}}) - \sigma(t)}{\sigma(t_{\text{sat}}) - \sigma(t_{\text{on}})} \quad (15)$$

is presented in a semi-logarithmic scale. Here $\sigma(t_{\text{on}})$ represents the value of conductivity at the instant of turning the light on and $\sigma(t_{\text{sat}})$ is the saturated conductivity under illumination. The observed non-exponential transients of the normalized relative photoconductivity may be properly described in terms of the stretched-exponential function (cf equation (1)).

In figures 3(d)–(f) the response data (defined as the growth rate of the normalized relative conductivity $f(t) = -\frac{d\Delta\sigma(t)}{dt}$) are shown in a log–log scale. In this representation, within

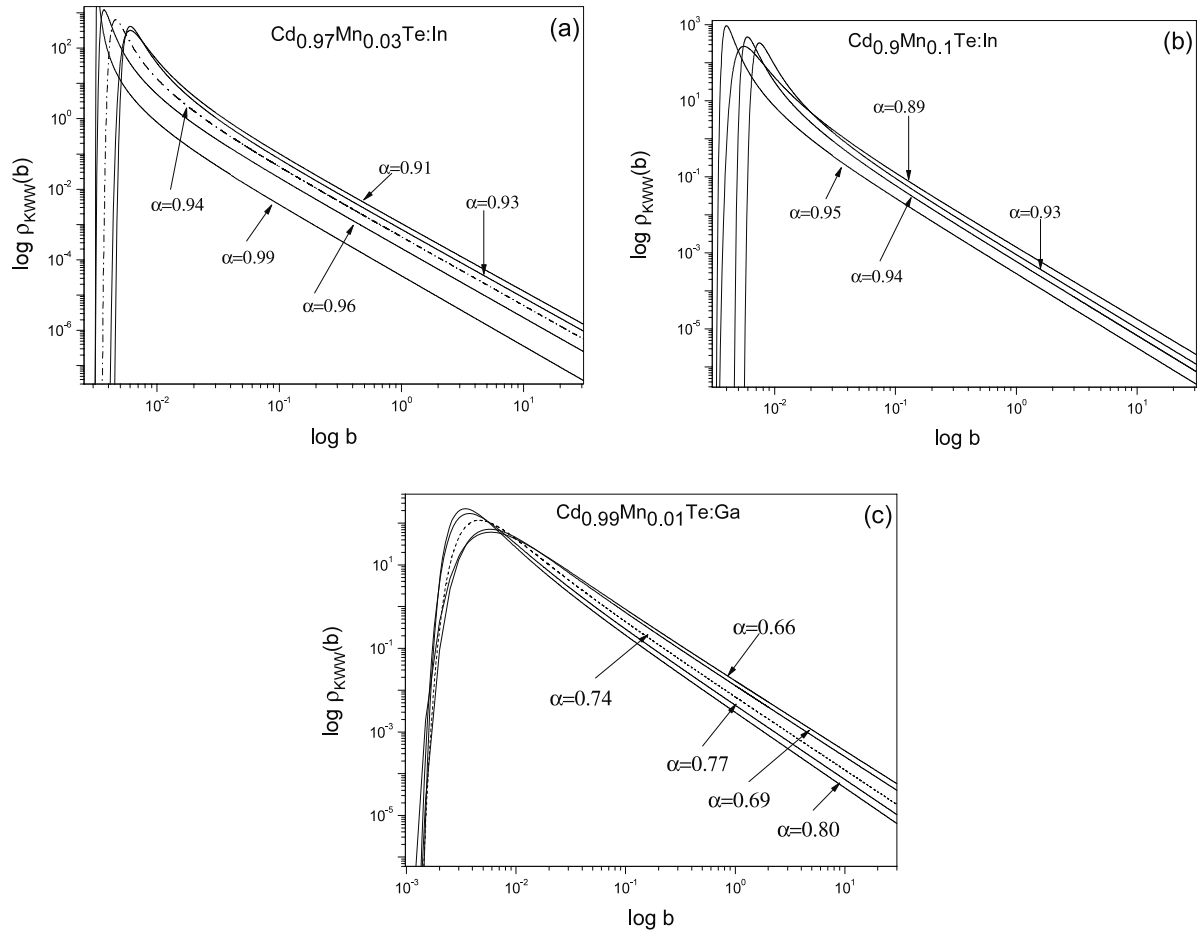


Figure 5. α -stable densities of the DX centers' relaxation rates for various values of the parameter $\alpha \in (0, 1)$. The densities decay as $b^{-\alpha-1}$ for $b \rightarrow \infty$.

the short-time range, a time dependence of $f(t) \sim t^{\alpha-1}$ is observed as a straight line (cf the data in the ellipses). This is the fingerprint of the power-tail property (10) of the relaxation rate pdf. This power-law property has been observed for gallium- and indium-doped samples and for various photon fluxes. It can be noted that, within the whole measured time range, the response function can be perfectly fitted by the stretched-exponential response function.

In table 1 values of the parameters, obtained as a result of fitting the experimental data by means of the stretched-exponential function, are reported. It was found that, regardless of donor types, the values of the stretching exponent α decrease linearly with increasing photon flux (see figure 4). For indium-doped material the values of α fall in the range of (0.89–0.99), whereas for gallium-doped samples they fall in the range of (0.66–0.80). It was discussed in [11] that the value of the stretching exponent reflects the internal stochastic characteristic of the investigated medium. The material is more dispersive, i.e. the defect relaxation rates are more spread, when α takes smaller values. For α approaching 1, the defects' relaxation rates are focused around the mode of their distribution.

Within the stochastic approach to relaxation processes it can be shown that the observed stretched-exponential

Table 1. The values of fitting parameters: stretching exponent α and time constant $\tau = 1/A$ for various photon fluxes.

Photon flux (arb. units)	Cd _{0.97} Mn _{0.03} Te:In		Cd _{0.9} Mn _{0.1} Te:In		Cd _{0.99} Mn _{0.01} Te:Ga	
	α	1/A (s)	α	1/A (s)	α	1/A (s)
2	0.99	345	0.95	213	—	—
3	—	—	—	—	0.80	282
4	0.96	244	0.94	137	0.77	144
5	—	—	—	—	0.74	107
6	0.94	175	0.93	114	—	—
7	—	—	—	—	0.69	66
8	—	—	—	—	0.66	41
9	0.91	120	0.89	100	—	—

behavior of the photoconductivity transients in indium- and gallium-doped Cd_{1-x}Mn_xTe may be related to an α -stable relaxation rate distribution of the photoionized defects—the DX centers [11]. In figure 5 the KWW relaxation rate distribution functions $\rho_{KWW}(b)$ for indium- and gallium-doped Cd_{1-x}Mn_xTe are plotted in a log–log scale. The values of relaxation parameters used for density calculations are given in table 1. Note that the smaller the value of α is, the heavier the tail of the density becomes. Hence, the tails of the densities decay slower for gallium-doped samples. The

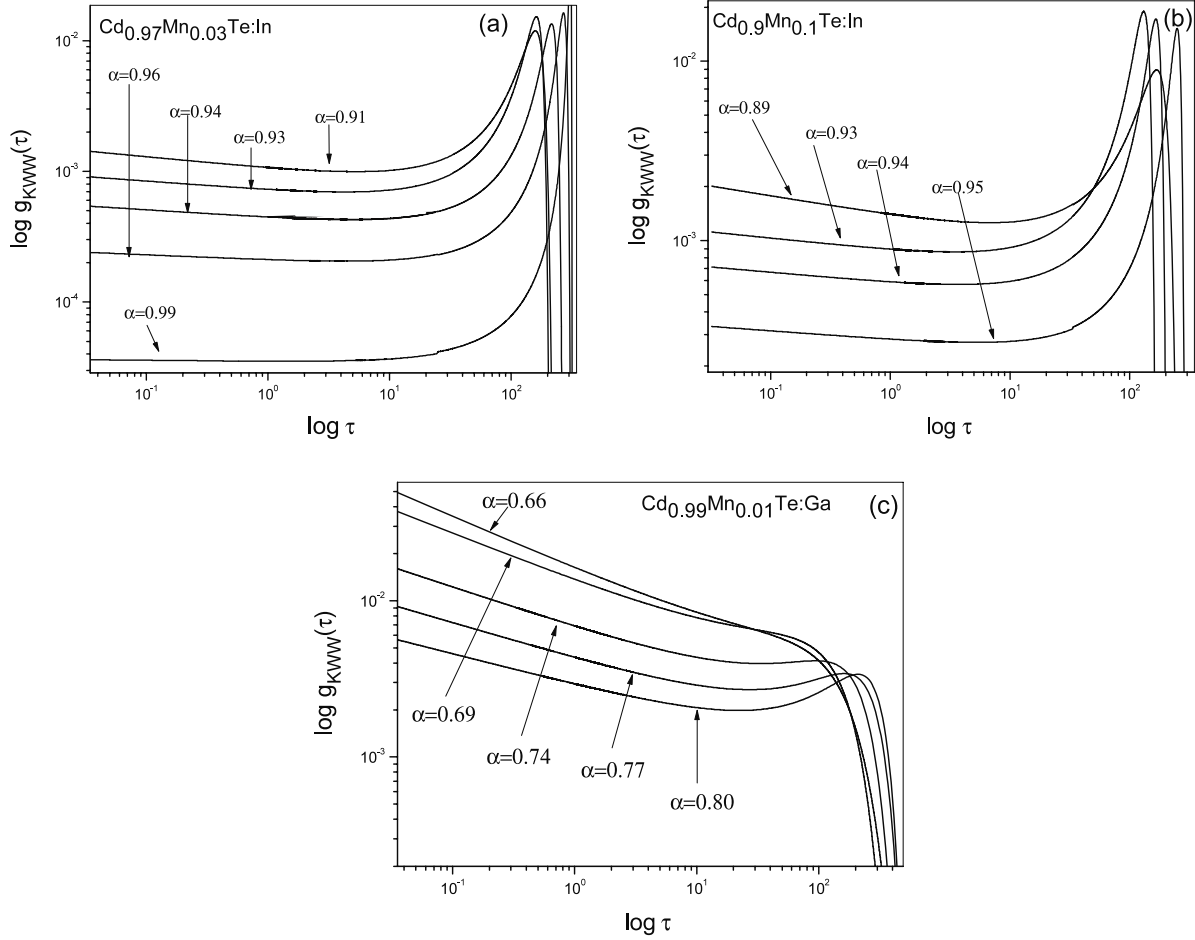


Figure 6. Densities of the DX centers relaxation times. Note the power-law property $\tau^{\alpha-1}$ for $\tau \rightarrow 0$.

power-law asymptotic property observed for large b remains in agreement with those described by formula (10).

According to the fact that the relaxation rate density and the relaxation time density are related, it follows from (6), (8) and (9) that the relaxation time pdf may also be given in terms of a series representation, i.e.

$$g(\tau) = \frac{1}{\pi\tau} \sum_{n=1}^{\infty} (-1)^{n+1} \frac{\Gamma(n\alpha + 1)}{n!} (\tau A)^{n\alpha} \sin(\pi n\alpha)$$

for $\tau \rightarrow 0$ (16)

and

$$g(\tau) = \frac{1}{\tau} \left[\frac{B(\alpha)\lambda(\alpha)}{2\pi(1-\alpha)} \right]^{\frac{1}{\alpha}} (\gamma\tau)^{\frac{\lambda(\alpha)}{2}} \exp[-B(\alpha)(\gamma\tau)^{\lambda(\alpha)}],$$

for $\tau \rightarrow \infty$ (17)

where

$$B(\alpha) = (1-\alpha)\alpha^{\frac{\alpha}{1-\alpha}} \left(\cos\left(\frac{\pi\alpha}{2}\right) \right)^{-\frac{1}{1-\alpha}}, \quad \lambda(\alpha) = \frac{\alpha}{1-\alpha}$$

and

$$A = \frac{\gamma}{\left[\cos\left(\frac{\pi\alpha}{2}\right) \right]^{\frac{1}{\alpha}}}, \quad (18)$$

is one of the KWW fitting parameters (cf equation (1)), which is understood as an inverse of characteristic material

Table 2. The values of parameter γ for various photon fluxes.

Photon flux (arb. units)	Cd _{0.93} Mn _{0.07} Te:In	Cd _{0.9} Mn _{0.1} Te:In	Cd _{0.99} Mn _{0.01} Te:Ga
	γ (s ⁻¹)	γ (s ⁻¹)	γ (s ⁻¹)
2	0.00004	0.0003	—
3	—	—	0.0008
4	0.0002	0.0006	0.0018
5	—	—	0.0027
6	0.0005	0.0008	—
7	—	—	0.0050
8	—	—	0.0088
9	0.0010	0.0014	—

time constant. According to equation (18) the value of A is determined by the value of the stretching exponent α and some positive constant γ . In table 2 values of the parameter γ obtained for all the investigated samples are reported. It would appear that the value of this parameter depends on the donor type in the investigated Cd_{1-x}Mn_xTe. It takes larger values for gallium-doped samples. For indium-doped material values of γ are smaller for samples with smaller indium content. Unfortunately, the physical meaning of this constant is not clear for us at the moment.

In figure 6 the relaxation time $g_{KWW}(\tau)$ pdfs, corresponding to the relaxation rate densities depicted in figure 5, are

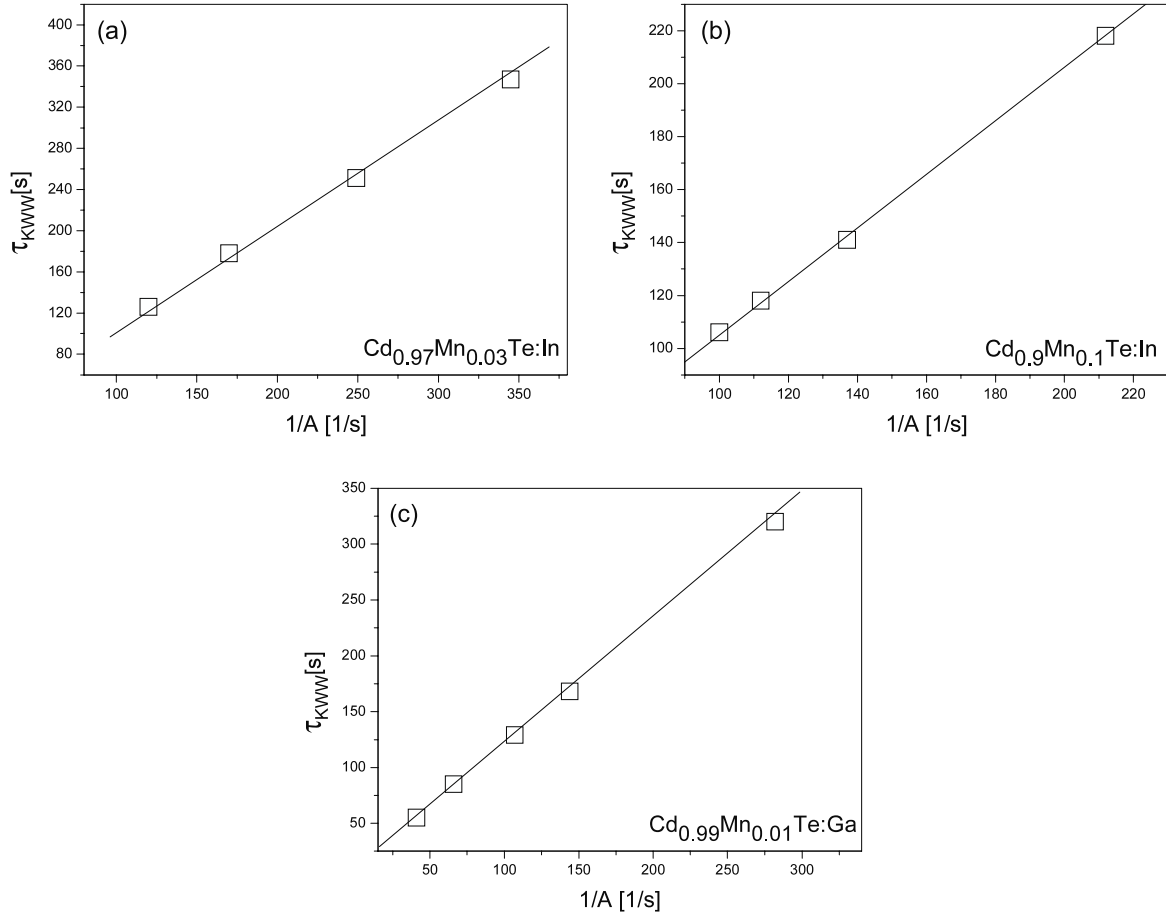


Figure 7. The expected value of the KWW relaxation time versus $1/A$. The value of A results from fitting the experimental data by means of the stretched-exponential function (1).

shown in a log–log scale. In contrast to $\rho_{KWW}(b)$, the relaxation time pdf does not exhibit the power-law decay for large values of τ . The power-tail behavior $\tau^{\alpha-1}$ is observed as a linear dependence solely for $\tau \rightarrow 0$.

Both considered densities exhibit various asymptotic behavior. Therefore to obtain the complete information concerning the random properties of the relaxing defects it is useful to look at the system in terms of both the representations (4) and (5). The proposed approach allows us also to calculate the expected value of the effective relaxation time. Taking into consideration equation (12) and relationship (6) one can find the expected value of the relaxation time:

$$\tau_{KWW} = \langle T_{KWW} \rangle = \int_0^\infty \tau g_{KWW}(\tau) d\tau, \quad (19)$$

even without the explicit knowledge of $\rho_{KWW}(b)$. Namely, since from (6)

$$\rho_{KWW}(b) = \frac{1}{2\pi i} \int_{-i\infty}^{i\infty} e^{bt} \Phi_{KWW}(t) dt \quad (20)$$

where $b = 1/\tau$, we get from (12) that

$$\tau_{KWW} = \int_0^\infty \frac{1}{b} \left[\frac{1}{2\pi i} \int_{-i\infty}^{i\infty} e^{bt} \Phi_{KWW}(t) dt \right] db. \quad (21)$$

Moving the b^{-1} term inside the integral over dt , interchanging the order of integration and moving the $\Phi(t)$ term outside the integration over db yields

$$\tau_{KWW} = \int_0^\infty e^{-(At)^\alpha} dt = \frac{1}{A} \Gamma\left(\frac{1}{\alpha} + 1\right), \quad (22)$$

which bonds the expected value of the effective relaxation time τ_{KWW} with the values of the KWW fitting parameters α and A . In figure 7 the expected value of the relaxation time versus the inverse of A is depicted. The experimental results remain in agreement with the demonstrated theoretical calculation, i.e. the linear dependence of τ_{KWW} on $1/A$ is observed for all the analyzed materials. In table 3 the expected value of the relaxation time τ_{KWW} and parameter $\Gamma(\frac{1}{\alpha} + 1)$ for different photon fluxes is presented. It is clear from the table that the relaxation time gets shorter with increasing photon flux. This tendency, observed for all the studied samples, stays in agreement with our physical intuition. Higher photon flux results in quicker ionization of the defects. Furthermore, the relaxation time takes smaller values in the case of gallium-doped samples as compared to indium-doped ones. Moreover, the smaller expected value of the effective relaxation time is related to the $\text{Cd}_{1-x}\text{Mn}_x\text{Te:In}$ samples with higher indium content. Values of the parameter $\Gamma(\frac{1}{\alpha} + 1)$ given in table 3 were determined in two ways: as the gamma function value

Table 3. Parameter $\Gamma(\frac{1}{\alpha} + 1)$ and expected values τ_{KWW} of the relaxation time for various photon fluxes. Values of τ_{KWW} were calculated using equation (22).

Photon flux (arb. units)	Cd _{0.93} Mn _{0.07} Te:In			Cd _{0.9} Mn _{0.1} Te:In		
	τ_{KWW} (s)	$\Gamma(\frac{1}{\alpha} + 1)$	Slope coefficient	τ_{KWW} (s)	$\Gamma(\frac{1}{\alpha} + 1)$	Slope coefficient
2	347	1.00 ± 0.01	1.02 ± 0.04	218	1.02 ± 0.01	1.03 ± 0.04
4	249	1.02 ± 0.01		141	1.03 ± 0.01	
6	180	1.03 ± 0.01		118	1.03 ± 0.01	
9	126	1.05 ± 0.01		106	1.06 ± 0.01	
Cd _{0.99} Mn _{0.01} Te:Ga						
Photon flux (arb. units)	τ_{KWW} (s)	$\Gamma(\frac{1}{\alpha} + 1)$	Slope coefficient			
3	320	1.13 ± 0.01	1.16 ± 0.08			
4	168	1.17 ± 0.02				
5	129	1.20 ± 0.02				
7	85	1.28 ± 0.02				
8	55	1.34 ± 0.02				

and as the slope coefficient of linear fit to the τ_{KWW} versus $1/A$ data.

For indium-doped samples the value of $\Gamma(\frac{1}{\alpha} + 1)$ slightly changes with varying photon flux. For gallium-doped material differences would seem to be more significant. Values of this parameter obtained from calculations remain in agreement within the error range of these which were determined as the slope coefficients of the τ_{KWW} versus $1/A$ dependence.

5. Conclusions

In this paper the properties of the effective relaxation rate and relaxation time distributions, underlying the stretched-exponential relaxation pattern observed in gallium- and indium-doped Cd_{1-x}Mn_xTe, have been discussed. It was shown that the stretched-exponential relaxation function, which properly describes photoconductivity build-ups in these materials, can be expressed by means of the Laplace transform of an α -stable distribution of the effective DX centers' relaxation rate. The asymptotic properties of the heavy-tailed relaxation rate pdf have been straightforwardly related to the short-time power-law property of the measured photoconductivity response transients. Furthermore, the relation between the DX centers' relaxation rate and the relaxation time densities was brought into the limelight. For the first time the effective relaxation time pdfs were presented for Cd_{0.97}Mn_{0.03}Te:In, Cd_{0.9}Mn_{0.1}Te:In and Cd_{0.99}Mn_{0.01}Te:Ga. It was emphasized that the heavy-tailed property of the DX centers' relaxation rate distribution yields the infinite mean value of effective relaxation rate. However, the relaxation time distribution does not possess the power-law tail for large values of time. Therefore, it is possible to calculate the mean value of the KWW relaxation time. The relation between the expected value of the KWW relaxation time τ_{KWW} and the characteristic material time constant $1/A$ obtained from the data fitting was clarified. Summarizing, the

KWW relaxation time distribution approach gives additional information concerning the random characteristic of the DX centers in the studied materials.

Acknowledgment

The work has been financially supported by the European Union from the European Regional Development Fund project no. POIG.01.03.01-02-002/08.

References

- [1] Havriliak S Jr and Havriliak S J 1994 *J. Non-Cryst. Solids* **172-174** 297
- [2] Jonscher A K 1996 *Universal Relaxation Law* (London: Chelsea Dielectrics Press)
- [3] Kremer F 2002 *J. Non-Cryst. Solids* **305** 1
- [4] Jurlewicz A and Weron K 1999 *Cell. Mol. Biol. Lett.* **4** 55
- [5] Weron K, Jurlewicz A and Jonscher A K 2001 *IEEE Trans. Dielectr. Electr. Insul.* **8** 352
- [6] Jurlewicz A and Weron K 2002 *J. Non-Cryst. Solids* **305** 112
- [7] Jonscher A K, Jurlewicz A and Weron K 2003 *Contemp. Phys.* **44** 329
- [8] Szabat B, Weron K and Hetman P 2007 *J. Non-Cryst. Solids* **353** 4601
- [9] Trzmiel J, Placzek-Popko E, Wrobel J M, Weron K and Becla P 2008 *J. Phys.: Condens. Matter* **20** 335218
- [10] Trzmiel J, Placzek-Popko E, Weron K, Szatkowski J and Wojtyna E 2008 *Proc. XXXVII Int. School on Phys. of Semiconducting Compounds (Jaszowiec, June 2008); Acta Phys. Pol. A* **114** 1417
- [11] Trzmiel J, Weron K and Placzek-Popko E 2008 *J. Appl. Phys.* **103** 114902
- [12] Bötcher C J and Bordewijk P 1978 *Theory of Electric Polarisation* vol 2 (Amsterdam: Elsevier)
- [13] Feller W 1996 *An Introduction to Probability Theory and its Applications* (New York: Wiley)
- [14] Zolotariev V M 1986 *One-Dimensional Stable Distributions* (Providence, RI: American Mathematical Society)